

IDENTIFICATION AND CONTROL OF SALTWATER INTRUSION BY ADR APPROACH IN THE COASTAL AQUIFERS OF TUTICORIN, INDIA

GLORY SELVAMANO, J.^{1*} – PRINCE ARUL RAJ, G.² – JEYANTHI, J.³

¹*Sardar Raja College of Engineering, Alangulam-627808, Tamilnadu, India*

²*Karunya Institute of Technology and Sciences, Coimbatore-641114, Tamilnadu, India*

³*Government College of Technology, Coimbatore-641013, Tamilnadu, India*

**Corresponding author*

e-mail: gloryjason2007@gmail.com

(Received 13th Nov 2018; accepted 16th Jan 2019)

Abstract. Due to industrial growth and urbanisation, excessive usage of groundwater resulted in a problem of saltwater intrusion in Tuticorin, India where control and management is very much essential. In the present study, groundwater samples are collected and analysed from 38 observation wells in years 2014 and 2018. Thirteen parameters namely pH, Electrical Conductivity (EC), Total Dissolved Solids (TDS), Total Hardness (TH), Calcium (Ca²⁺), Magnesium (Mg²⁺), Sodium (Na⁺) Potassium (K⁺), Bicarbonate (HCO₃⁻), Chloride (Cl⁻), Sulphate (SO₄²⁻) Nitrate (NO₃⁻) and Fluoride (F⁻) are determined and considered in calculating the Water Quality Index (WQI) based upon weighted arithmetic index method. Geographical information system (GIS) is used to interpolate water quality data by inverse distance weighted method. Experimental investigation indicates saltwater intrusion in the coastal aquifer of Tuticorin is due to excessive withdrawal of groundwater. Potential intrusion of saltwater is studied with respect to distance of observation wells from seashore. Finite Element Modelling of Flow (FEFLOW) is used to select the optimum pumping and recharge rate to control saltwater intrusion. A model is calibrated with hydraulic head measured using piezometer in the observation well, as well as salt concentration. The model is simulated using three different groundwater scenarios such as Abstraction, Recharge and combined Abstraction, Desalination Recharge (ADR) method. The simulation results depicted that the planned ADR system accomplishes significantly better than using abstraction or recharge well.

Keywords: *GIS, groundwater management, FEFLOW, hydraulic head, water quality index*

Introduction

Groundwater extraction is required in several coastal areas where the freshwater supply from surface sources is not sufficient. However, extreme groundwater abstraction may lead to intrusion of saltwater into the aquifer, henceforth salinity increases making the groundwater unfit for human intake (Rao et al., 2004). Saltwater contamination arises due to vertical movement across interconnected aquifers through open well or bore well (Barlow and Reichard, 2010). Jebastina and Prince Arulraj (2016) analysed groundwater and determined the quality changes due to silicate weathering and dissolution of carbonate. Assessment of groundwater quality plays a vital role in our society, predominantly concerning health (Sener et al., 2009). One of the important and easy methods for evaluating intrusion of saltwater in coastal areas is periodic analysis of groundwater chemistry (Todd, 1980). The information of hydrochemistry is significant to assess the groundwater quality in Coimbatore in which the groundwater is used for drinking, agriculture, and industrial purposes (Jebastina and Prince Arulraj, 2017). In recent years water quality index (WQI) has become an

essential method to assess the quality of groundwater. Tavassoli and Mohammadi (2017) assessed the vulnerability of groundwater based on WQI values. WQI method handles complex data of water quality parameter and provides simplified output to understand water quality problem. Idowu et al. (2016) used geographical information system (GIS) as a prevailing tool to assess vulnerability of seawater intrusion and effective management of Groundwater.

Todd (1974) discussed various methods of preventing saltwater from polluting groundwater sources including; decrease of pumping rates, repositioning of extraction wells, use of sub-surface walls, recharge of water by natural and artificial methods, abstraction of saline groundwater and any combination of above techniques. El Mokhtar et al. (2018) developed model for planning and management of sustainable use of groundwater resources in the coastal aquifer of Fum Al Wad, Morocco. Groundwater model evidenced that pumping of saline water from coastal aquifers would mitigate the rate at which saltwater flows into the aquifer so that quality of water improved. Hussain et al. (2015) suggested continuous Abstraction of brackish water, desalination and recharge techniques control saltwater intrusion effectively in coastal aquifers. Thomas et al. (2016) used simulation model to determine proper pumping strategy for the management of Coastal aquifers. Finite Element Modelling of Flow (FEFLOW) is a software used for groundwater modelling capable of simulating flow.

The main objective of this study is to evaluate the quality of groundwater using WQI in Tuticorin, India and thematically denote it using Geographical information system (GIS) for the better understanding of the current scenario at a glance. An effort has been made in the coastal aquifers of Tuticorin to protect the wells from seawater intrusion by FEFLOW code, using hydrogeological and hydro chemical data.

Location of the study area

The study area Tuticorin is situated in the southeast shoreline of Tamil Nadu, India and is positioned between 8° 19' to 9° 22' N latitude and 77° 40' to 78° 23' E longitude. The area is bound by the Gulf of Mannar in the east and Tirunelveli district, Tamil Nadu in the west. The main occupation of the people is agriculture. Many chemical industries, food processing industries, salt industries are situated in Tuticorin. Many industries are established after the construction of the port and Tuticorin became a district in the year 1986. After the formation, the economic development has been boosted and began to develop rapidly. Therefore, the urban expansion acquired in various areas of the district. The slope of the terrain is mild in the western part and flat in the eastern part. The location map of the study area is shown in *Figure. 1*.

Methodology

Sample collection

A total of 38 groundwater samples are collected from open and bore wells. The location of observation wells is shown in *Figure 2*. Each sample is collected in 1000 mL acid-washed polyethylene HDPE bottle. The bottle is fully filled with water such that no air bubble is stuck within the water sample. To avoid evaporation, the bottles are closed with double plastic caps. Precaution is also taken to prevent agitation of sample during transfer from field to the lab.

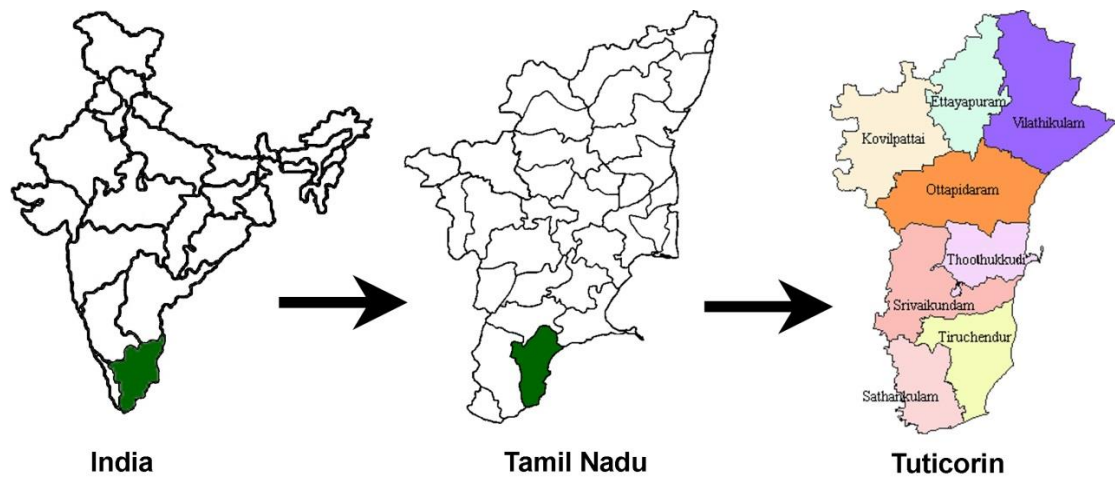


Figure 1. Location map of study area

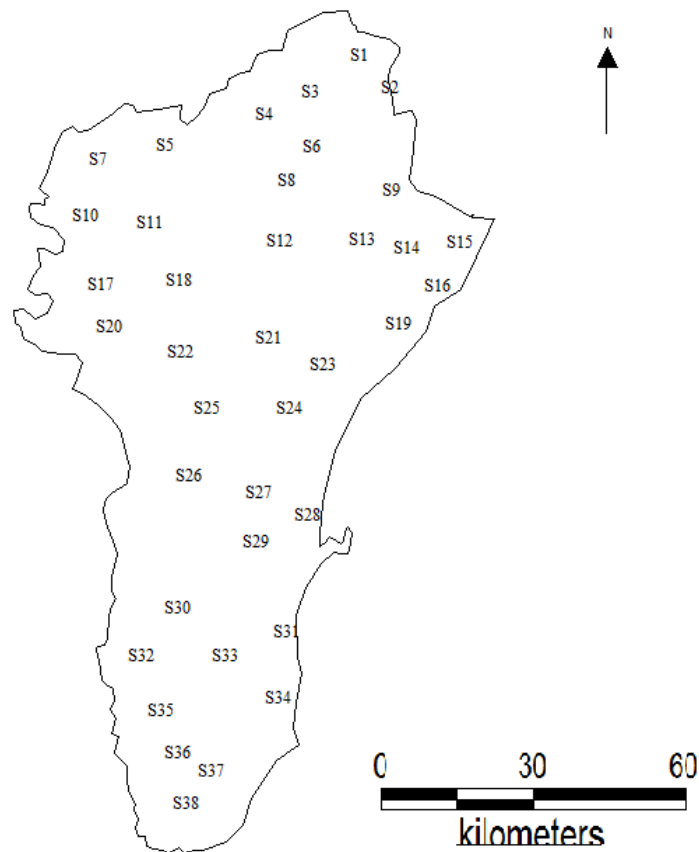


Figure 2. Location of observation wells

Laboratory measurements

The physico-chemical analysis was conducted using following methods and equipment as shown in *Table 1*.

Table 1. Method and instrument used in water quality analysis

S.No	Parameter	Method	Instrument/equipment
1.	pH	Electrometric	pH meter
2.	EC (electrical conductivity)	Electrometric	Conductivity meter
3.	TDS (total dissolved solids)	Electrometric	Conductivity meter
4.	TH (total hardness)	Titration by EDTA	-
5.	Ca ²⁺ (Calcium)	Titration by EDTA	-
6.	Mg ²⁺ (Magnesium)	Titration by EDTA	-
7.	Na ⁺ (Sodium)	Flame emission	Flame photometer
8.	K ⁺ (Potassium)	Flame emission	Flame photometer
9.	HCO ₃ ⁻ (Bicarbonate)	Titration by H ₂ SO ₄	-
10.	Cl ⁻ (Chlorine)	Titration by AgNO ₃	-
11.	SO ₄ ²⁻ (Sulphate)	Use wavelength of 420 nm	UV-VIS spectrophotometer
12.	NO ₃ ⁻ (Nitrate)	Use wavelength of 220 nm	UV-VIS spectrophotometer
13.	F ⁻ (Fluoride)	Ion-selective electrode (ISE)	pH meter

All concentrations are denoted in milligrams per litre (mg/L), excluding the pH and EC

Determination of water quality index (WQI)

To calculate WQI, thirteen parameters namely pH, EC, TDS, TH, Ca²⁺, Mg²⁺, Na⁺, K⁺, HCO₃⁻, Cl⁻, SO₄²⁻, NO₃⁻ and F⁻ are considered into account. The following few steps are followed in calculating WQI.

Parameter selection

The selection of parameters depends on several aspects, such as the purpose of the index, the importance of the parameter, and the availability of data (Stigter et al., 2006). For the assessment of drinking water quality, priority should be given to those parameters which are known to be important to health and to be present in significant concentrations in the water source (Ramesh et al., 2010). Table 2 gives the details of the weights and relative weights assigned to various parameters.

Table 2. Weights for various parameters

Water quality parameter	Units	WHO (2017)		Weight (W)	Relative weight (W _R)
		Most desirable limit	Maximum allowable limit		
pH	-	6.5	8.5	4	0.09
EC	µs/cm	780	3125	-	-
HCO ₃	mg/L	-	300	1	0.03
TDS	mg/L	500	1500	5	0.11
F	mg/L	-	1.5	5	0.11
Cl	mg/L	200	600	5	0.11
NO ₃	mg/L	45	-	5	0.11
SO ₄	mg/L	200	400	5	0.11
Na	mg/L	-	200	4	0.09
Ca	mg/L	75	200	3	0.07
Mg	mg/L	30	150	3	0.07
K	mg/L	-	10	2	0.05
TH	mg/L	300	600	2	0.05
				ΣW = 44	ΣW _R = 1

Drinking water quality standards given by the World Health Organization (WHO, 2017)

Weight assignment

The assignment of weight to water quality parameters is to represent the importance of each parameter in the overall water quality. Higher weightage implies greater importance of the variable with respect to public health (Song and Kim, 2009). Therefore, each of the selected parameters has been given a weight (W) 1 to 5, depending on their importance. The chosen weights are tabulated in *Table 2*. These weights are assumed based on the data available from previous studies (Serrekawo and Karoppannan, 2018; Ramakrishnaiah et al., 2009; Gebrehiwot et al., 2011; Kalpana et al., 2014).

Relative weight calculation

Relative weight (W_R) can be determined by dividing the individual weight of each parameter (W_I) by the sum of weight of all selected parameters (W) shown in *Equation 1*.

$$W_R = \frac{W_I}{W} \quad (\text{Eq.1})$$

where W_R is the relative weight, W_I is the weight of the parameter under consideration.

Quality rating calculation

The fourth step is the calculation of quality rating (Q_I) for each parameter, is given in *Equation 2*.

$$Q_I = \frac{C_I}{S_I} \times 100 \quad (\text{Eq.2})$$

where Q_I is quality rating, C_I (mg/L) is the concentration of each parameter in water sample, and S_I (mg/L) is the Bureau of Indian standard for chemical parameter.

Sub-index calculation

The sub-index for each chemical parameter is determined using *Equation 3*.

$$S_I = W_R \times Q_I \quad (\text{Eq.3})$$

S_I is the sub-index of the i th parameter. It combines its quality rating as well as its assigned weight.

Calculation of water quality index

The overall WQI is calculated by summation of all sub index values of each groundwater sample as follows (*Eq. 4*):

$$WQI = \sum S_I \quad (\text{Eq.4})$$

Classification of water quality index

Higher WQI values indicate worse water quality, and lower values indicate excellent water quality. The detail description of WQI range and its classification is given in Table 3.

Table 3. Classification of WQI values

WQI range	Category of water
<50	Excellent
50–100	Good
100–200	Poor
200–300	Very poor
>300	Unfit for drinking purpose

GIS analysis

GIS is an effective method for spatial analysis and integration of the data to derive needed outputs and modelling. GIS can be beneficial for taking fast conclusions as graphical illustration would make visualization easy for policy makers. The study area of Tuticorin district is digitized from the survey of India toposheet using QGIS. The exact locations of observation wells are determined in the field using GPS and the precise longitudes and latitudes of observation wells are imported in GIS platform. Inverse Distance Weighted (IDW) interpolation method was used for spatial modelling of WQI and the parameter values are classified according to Table 3.

Model development (FEFLOW)

The first step in FEM analysis is the generation of mesh that fills the envisioned model domain with elements as shown in Figure 3. Based on the finite-element mesh, initial hydraulic head, boundary conditions and material properties are defined as given in Table 4.

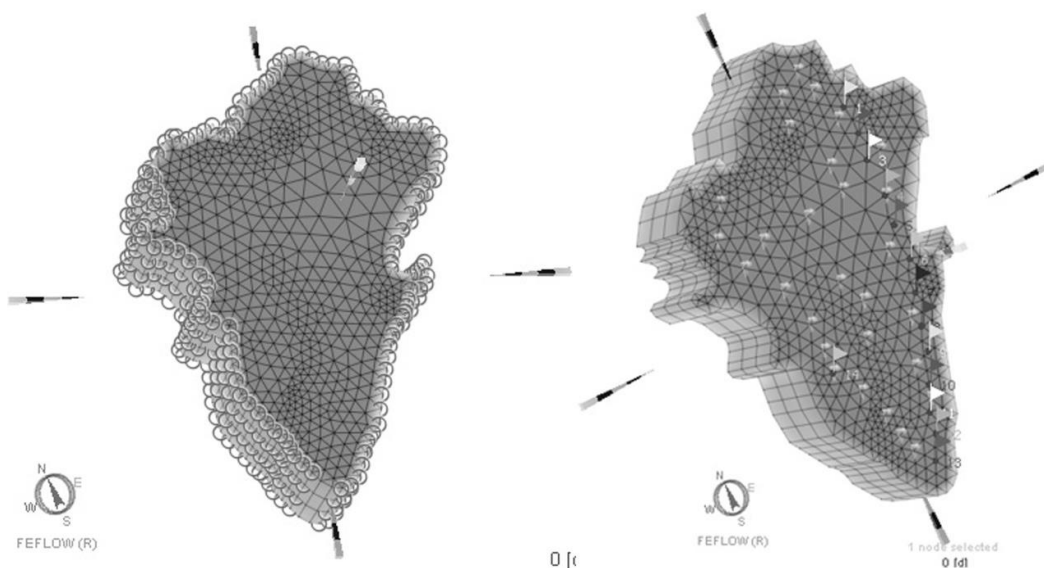


Figure 3. Generation of finite element mesh

Table 4. Data used for model development

Parameter	Value
Physical parameters	
Mesh	
Element type	Triangle prism
Mesh element	3351
Mesh node	2496
Number of layer	1
Number of slice	2
Total model boundary areas	4621 km ²
Materials properties and boundary conditions (BC)	
Hydraulic conductivity K_x, K_y, K_z	4.5×10^{-4} m/s, 4.5×10^{-4} m/s, 1.5×10^{-4} m/s
Specific storage (fluid flux)	.002
Total porosity	.35
Longitude dispersivity	1
Transverse dispersivity	0.1 m
Density ratio	1025 kg/m ³
Constant head	0 m
Recharge concentration	0 mg/L
Constant head concentration	35000 mg/L
Initial concentration	20.22
Initial head	1.011 m

The model is calibrated by changing the aquifer properties and the boundary conditions in order to obtain a model appropriate to simulate the groundwater flow and the mass concentration distribution, within the calibration target. In the calibration process, a trial and error technique is carried out in order to reduce the variance between the simulated and the measured values. Once the model is calibrated; it is run to verify various scenarios as shown in *Table 5* where the extrapolative simulations are performed to minimize saltwater intrusion in the unconfined aquifer.

Table 5. Three scenarios used for model simulation

Simulation	Description
Scenario A	Abstraction of saline water 1000 m ³ /day
Scenario B	Recharge of treated water at the rate of 500 m ³ /day
Scenario C	Abstraction of saline water 1000 m ³ /day, desalination and recharge of treated water at the rate of 500 m ³ /day

Results

Laboratory measurements

The water quality characteristics of the groundwater samples during the year 2014 and 2018 are determined and the values are given in *Tables 6* and *7*.

Table 6. Physico-chemical values in 2014

Well No	Latitude	Longitude	pH	EC	TDS	TH	Ca	K	Na	Mg	HCO ₃	Cl	SO ₄	F	NO ₃	WQI 2014
S1	09°13'47"	78°08'12"	7.5	1360	763	370	54	9	145	57	342	220	33	0.38	17	130
S2	09°14'09"	78°01'50"	8	1440	823	420	60	4	145	66	354	149	154	0.38	15	121
S3	09°17'47"	78°03'56"	8.5	1190	749	305	84	3	124	23	73	21	442	0.65	1	86
S4	09°10'45"	77°52'25"	8.3	770	458	235	48	7	69	28	142	99	65	0.36	12	77
S5	09°08'30"	78°02'15"	8	3070	1985	550	80	12	460	85	366	355	624	1.04	42	258
S6	09°08'57"	77°42'10"	8.8	2930	1612	540	108	2	414	66	641	482	192	1.14	2	254
S7	09°09'00"	77°59'54"	7.8	1270	755	330	42	7	145	55	336	124	154	1.09	14	116
S8	09°07'45"	78°10'07"	8.2	3950	2290	770	148	5	552	97	647	709	384	1.57	16	362
S9	09°08'40"	77°47'15"	7.7	1410	1045	810	152	23	177	104	232	234	68	0.32	38	179
S10	09°04'30"	77°48'30"	8.8	690	399	185	8	14	69	40	155	53	96	0.26	4	63
S11	09°06'00"	78°00'40"	7.7	3610	2257	820	296	12	460	19	311	837	154	0.15	73	375
S12	08°33'00"	78°01'00"	8.2	740	394	280	40	4	41	44	74	170	29	0.46	5	89
S13	09°04'00"	78°10'35"	8.5	1730	1028	400	60	2	225	61	354	191	288	0.78	3	145
S14	09°13'47"	78°08'12"	8.6	2600	1606	370	96	16	442	32	689	326	216	0.63	27	215
S15	09°00'10"	78°11'50"	7.9	550	296	235	40	4	20	33	203	21	41	0.56	3	51
S16	09°03'35"	77°44'50"	8.6	1520	936	230	16	7	253	46	293	170	214	1.4	16	136
S17	08°59'40"	77°51'38"	7.9	730	425	285	50	9	35	39	109	117	27	0.29	18	81
S18	09°00'00"	77°58'00"	8	1610	966	240	20	1	276	46	421	206	144	1.02	14	139
S19	09°03'00"	77°54'00"	7.6	2330	1527	350	48	108	350	56	470	340	173	0.58	49	245
S20	09°01'10"	78°02'45"	8.4	2100	1376	260	40	88	331	39	439	234	264	1.48	35	212
S21	08°56'40"	77°52'00"	8.4	1740	1060	370	28	121	161	73	366	255	115	0.22	27	199
S22	08°54'45"	78°01'25"	7.6	3050	1752	1320	240	37	78	175	238	709	96	0.33	67	353
S23	08°52'30"	78°02'15"	7.5	2540	1598	540	100	66	304	70	329	404	178	0.1	70	252
S24	08°51'38"	77°54'00"	7.9	2530	1504	560	80	78	290	87	537	390	192	0.41	26	250
S25	08°47'25"	77°52'15"	8.6	590	315	200	42	20	32	23	212	32	25	0.17	2	55
S26	08°48'35"	78°01'25"	7.5	880	503	260	360	37	368	87	178	465	336	0.23	59	100
S27	08°48'00"	78°10'00"	8.2	250	145	100	24	3	10	10	59	28	22	0.35	2	34
S28	08°44'12"	77°59'45"	8.2	330	215	95	22	2	35	10	54	35	29	0.8	11	45
S29	08°38'00"	77°55'00"	8.4	660	391	170	34	13	69	21	151	82	48	0.2	6	66
S30	08°34'30"	78°05'45"	8	1550	914	320	24	100	161	63	445	191	125	1.45	6	178
S31	08°34'40"	77°49'15"	8.8	2530	1459	460	76	16	368	66	427	475	192	1.07	8	243
S32	08°26'40"	78°00'32"	8	2230	1302	240	48	18	391	29	702	255	192	1.03	4	178
S33	08°29'00"	78°01'30"	8	530	328	155	34	59	23	17	218	18	10	0.36	7	67
S34	09°05'00"	78°05'00"	8.3	480	249	125	18	2	55	19	211	7	13	0.86	1	43
S35	08°27'00"	78°01'00"	8.2	1470	799	420	48	11	143	73	214	347	58	0.6	3	164
S36	09°12'54"	78°12'30"	8	980	563	305	50	13	87	44	244	152	63	0.79	7	106
S37	08°25'00"	78°57'00"	7.8	830	473	340	64	4	32	44	114	131	43	0.16	19	86
S38	08°24'30"	77°52'00"	8.2	1090	616	300	50	7	115	42.5	293	181	35	0.74	9	142

Table 7. Physico-chemical values in 2018

Well No	Latitude	Longitude	pH	EC	TDS	TH	Ca	K	Na	Mg	HCO ₃	Cl	SO ₄	F	NO ₃	WQI 2018
S1	09°13'47"	78°08'12"	8.2	1450	888	255	42	19	212	36	293	209	71	0.09	34	133
S2	09°14'09"	78°01'50"	8.2	1600	1022	430	92	20	166	49	329	163	125	0.06	55	250
S3	09°17'47"	78°03'56"	7.6	2640	1559	740	184	23	258	68	354	532	204	0.12	25	266
S4	09°10'45"	77°52'25"	8.2	610	352	165	28	4	67	23	207	28	27	0.23	11	50
S5	09°08'30"	78°02'15"	7.9	2680	1568	510	144	10	396	36	683	425	72	0.16	32	260
S6	09°08'57"	77°42'10"	8.1	190	99	80	18	1	7	9	74	7	7	0.32	1	24
S7	09°09'00"	77°59'54"	8.8	2040	1235	200	40	16	368	24	500	220	125	0.08	39	155
S8	09°07'45"	78°10'07"	8.2	3180	1886	670	72	47	414	119	268	737	250	0.06	25	335
S9	09°08'40"	77°47'15"	8.1	310	188	105	26	5	23	10	69	35	10	0.4	8	40
S10	09°04'30"	77°48'30"	8.2	920	555	210	46	7	113	23	299	67	42	0.17	24	76
S11	09°06'00"	78°00'40"	7.4	1890	1138	620	148	14	166	61	256	383	61	0.21	40	201
S12	08°33'00"	78°01'00"	7.9	1050	686	370	94	11	74	33	153	96	216	0.21	19	99
S13	09°04'00"	78°10'35"	8.1	9310	5581	1200	100	7	1610	231	732	1914	1344	0.85	2	837

S14	09°13'47"	78°08'12"	8	5680	3268	1420	272	8	644	180	708	993	768	0.25	11	502
S15	09°00'10"	78°11'50"	8.1	3590	2125	660	40	11	552	136	403	695	456	0.92	8	338
S16	09°03'35"	77°44'50"	8.1	870	514	90	12	16	154	15	360	39	83	1.43	3	78
S17	08°59'40"	77°51'38"	8	120	73	40	8	7	7	49	35	14	6	0.43	1	32
S18	09°00'00"	77°58'00"	8.2	3150	1885	580	112	4	460	73	458	596	206	0.06	46	287
S19	09°03'00"	77°54'00"	8	250	145	100	24	7	10	10	99	7	10	0.07	4	28
S20	09°01'10"	78°02'45"	8.7	2970	1826	320	44	20	552	51	598	319	451	1.4	16	235
S21	08°56'40"	77°52'00"	8.2	1910	1136	340	32	3	294	63	500	248	165	0.51	18	160
S22	08°54'45"	78°01'25"	7.5	3380	1994	740	144	7	460	92	647	560	202	0.13	46	297
S23	08°52'30"	78°02'15"	8.1	1780	1068	490	68	19	173	78	281	305	160	0.12	28	175
S24	08°51'38"	77°54'00"	8.2	1380	786	250	54	5	207	28	488	152	71	0.11	6	108
S25	08°47'25"	77°52'15"	8.2	340	194	125	18	9	20	19	89	39	24	0.83	2	48
S26	08°48'35"	78°01'25"	8.2	990	599	230	24	63	92	41	256	121	84	0.46	10	114
S27	08°48'00"	78°10'00"	8.1	8410	5350	2120	36	7	1104	493	488	1773	1440	1.31	28	840
S28	08°44'12"	77°59'45"	8	970	560	210	18	6	124	40	244	121	83	0.4	10	88
S29	08°38'00"	77°55'00"	8.1	340	189	125	30	3	20	12	89	35	18	0.39	4	40
S30	08°34'30"	78°05'45"	8.2	1360	796	315	42	59	143	51	439	145	80	1.33	13	145
S31	08°34'40"	77°49'15"	8.2	840	499	100	12	4	147	17	217	60	62	0.66	14	68
S32	08°26'40"	78°00'32"	8.2	2140	1227	500	112	9	276	53	525	376	112	0.35	6	199
S33	08°29'00"	78°01'30"	7.8	1390	835	445	120	8	117	35	177	273	75	0.2	27	147
S34	09°05'00"	78°05'00"	8.2	490	286	210	54	4	20	18	108	60	50	0.32	3	55
S35	08°27'00"	78°01'00"	8	2150	1288	300	36	63	336	51	580	305	81	1.28	28	211
S36	09°12'54"	78°12'30"	8	470	274	110	16	6	58	17	129	53	30	0.09	3	46
S37	08°25'00"	78°57'00"	8.2	780	441	220	42	16	74	28	197	106	26	1.03	6	87
S38	08°24'30"	77°52'00"	8.2	1350	816	305	58	11	173	39	171	266	78	0.44	24	142

The water quality characteristics of the groundwater samples during the year 2014 and 2018 is statistically analysed and the results such as maximum, minimum, mean and standard deviation values are given in *Table 8*.

Table 8. Statistical measures such as minimum, maximum, mean and standard deviation in 2014 and 2018

Water quality parameters	Jan 2014				Jan 2018			
	Min	Max	Mean	SD	Min	Max	Mean	SD
pH	7.4	8.8	8.09	0.25	7.5	8.8	8.12	0.38
EC	120	9310	1972.89	2028.29	250	4180	1662.11	1045.56
HCO ₃ ⁻	35	732	328.93	199.79	54	702	311.63	175.17
TDS	73	5581	1182.39	1236.79	145	2503	996.74	637.78
F ⁻	0	1	0.46	0.43	0	2	0.64	0.42
Cl ⁻	7	1914	328.34	430.94	7	865	253.03	224.93
NO ₃ ⁻	1	55	17.89	14.64	1	73	19.42	20.54
SO ₄ ²⁻	6	1440	194.08	322.85	10	624	145.63	133.62
Na ⁺	7	1610	265.55	317.25	10	552	196.18	154.98
Ca ²⁺	8	272	64.79	56.65	8	360	74.53	75.39
Mg ²⁺	5	493	62.32	86.10	10	175	52.34	31.98
K ⁺	1	63	14.71	16.17	1	121	24.84	33.06
TH	40	2120	418.42	412.23	95	1320	401.71	277.38

The values of water quality characteristics like pH, EC, HCO₃⁻, TDS, F⁻, Cl⁻, NO₃⁻, SO₄²⁻, Na⁺, Ca²⁺, Mg²⁺, K⁺ and TH in 2014 and 2018 are compared with drinking water quality norms recommended by WHO (2017) and the samples beyond allowable limit during the years 2014 and 2018 are given in *Table 9*.

Table 9. Comparison of groundwater quality with WHO standards

Water quality parameter	Units	WHO (2017)		Samples exceeding allowable limit in 2014	Samples exceeding allowable limit in 2018
		Most desirable limit	Maximum allowable limit		
pH	-	6.5	8.5	2	6
EC	µs/cm	780	3125	17	19
HCO ₃	mg/L	-	300	16	20
TDS	mg/L	500	1500	16	17
F	mg/L	-	1.5	1	0
Cl	mg/L	200	600	11	13
NO ₃	mg/L	45	-	3	5
SO ₄	mg/L	200	400	2	5
Na	mg/L	-	200	15	16
Ca	mg/L	75	200	3	1
Mg	mg/L	30	150	1	3
K	mg/L	-	10	20	16
TH	mg/L	300	600	5	8

pH

A pH value 7 indicates neutral. If the value is lower than 7 it indicates acidity and higher than 7 indicates alkalinity. The values of pH ranges from 7.5 to 8.8 and 7.4 to 8.8 during 2014 and 2018 which specifies that the groundwater is alkaline in both 2014 and 2018 and some of the samples exceed the maximum permissible limits of WHO standards. The slight alkalinity is due to the existence of bicarbonate ions, which are formed by the free combination of CO₂ in water with the carbonates from the aquatic life, which affects the pH of the water (Azeez et al., 2000). The spatial distribution of pH is shown in *Figure 4* indicates all the samples are within the permissible limit of 6.5-8.5., except two samples in 2014 and six samples in 2018.

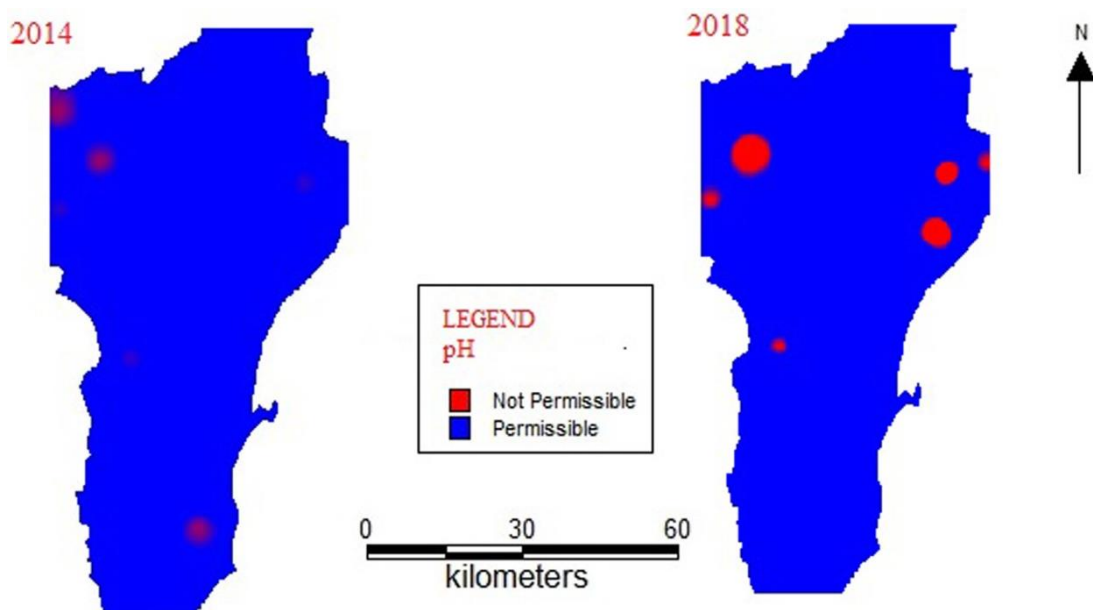


Figure 4. Spatial distribution of pH

Electrical conductivity

Electrical conductivity is the most significant parameter to delineate salinity hazard and suitability of water for irrigation purpose. The EC vary from 250 to 4180 $\mu\text{s}/\text{cm}$ and from 120 to 9310 $\mu\text{s}/\text{cm}$ during the years 2014 and 2018, respectively. The spatial distribution of EC is shown in *Figure 5*. Higher value of EC were noted during 2018 when compared to that of 2014. The classification of water salinity based upon Electrical conductivity shows that 45% in 2014 and 50% in 2018 falls within the permissible limit. To determine the salinity of groundwater, it is important to categorize the groundwater based on their EC values (Handa, 1969), which are represented in *Table 10*.

Table 10. Classification of waters based on EC (Handa, 1969)

EC ($\mu\text{s}/\text{cm}$)	Water salinity	2014		2018	
		Number of samples	Percentage of samples	Number of samples	Percentage of samples
0–250	Low	1	3	3	8
251–750	Medium	9	24	6	16
751–2250	High	17	45	19	50
2251–6000	Very high	11	20	8	21
6001–10000	Extremely high	-	-	2	5
10001–20000	Brines weakly concentrated	-	-	-	-
20001–50000	Brines moderately concentrated	-	-	-	-
50001–100000	Brines highly concentrated	-	-	-	-
>100000	Brines extremely highly concentrated	-	-	-	-
Total		38	100	38	100

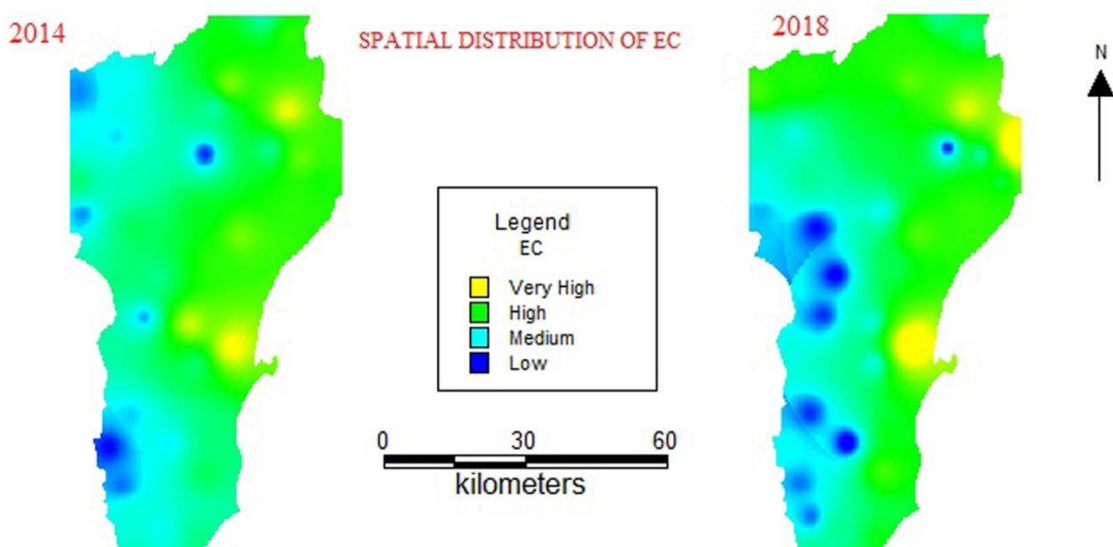


Figure 5. Spatial distribution of EC

Total dissolved solids

TDS of the groundwater are found to vary from 145 to 2503 mg/L during 2014 and 73 to 5581 mg/L during 2018. The Spatial Distribution of TDS is shown in *Figure 6*. Some groundwater samples having high value of TDS are may be due to presence of excess salts in the soil and also by manmade activities. Sewage waste from household may penetrate into the groundwater which also leads to raise in TDS values. To ascertain the groundwater, it is essential to categorize the groundwater based on their TDS values, which are presented in *Tables 11* and *12*, respectively.

Table 11. Classification of groundwater based on TDS (Davis, 1966)

Total dissolved solids (mg/L)	Classification	2014		2018	
		Number of samples	Percentage of samples	Number of samples	Percentage of samples
<500	Desirable for drinking	12	32	11	32
500–1000	Permissible for drinking	10	26	10	26
1000–3000	Useful for irrigation	16	42	14	37
>3000	Unfit for drinking and irrigation	0	-	3	8
Total		38	100	38	100

Table 12. Classification of groundwater based on TDS (Freeze and Cherry, 1979)

Total dissolved solids (mg/L)	Classification	2014		2018	
		Number of samples	Percentage of samples	Number of samples	Percentage of samples
<1000	Freshwater	16	42	15	39
1000–10000	Brackish water	22	58	23	61
10000–100000	Saline water	-	-	-	-
>100000	Brine water	-	-	-	-
Total		38	100	38	100

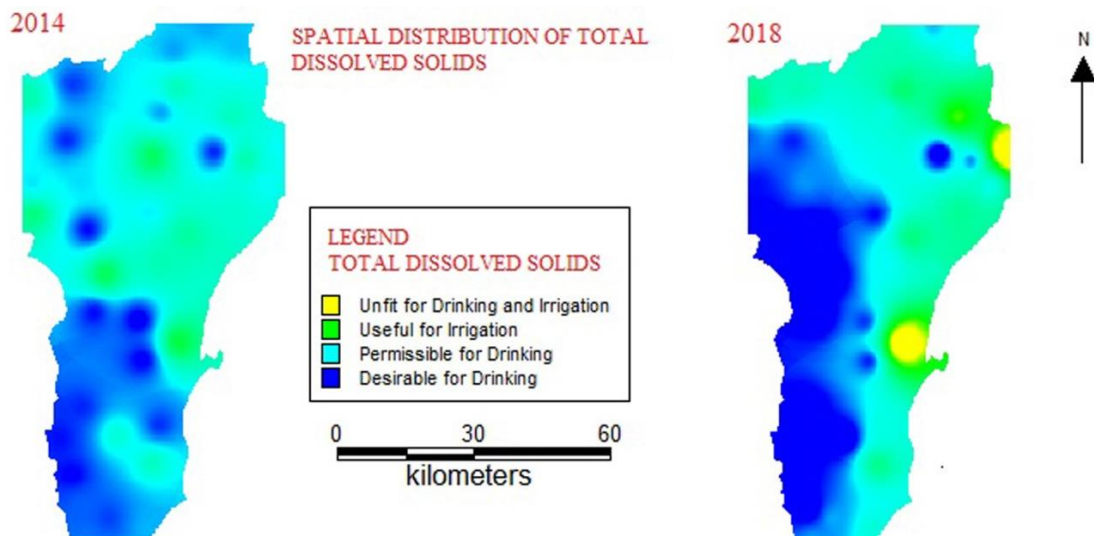


Figure 6. Spatial distribution of TDS

Total hardness

Total hardness is found to vary from 95 to 1320 mg/L with a mean value of 401.71 mg/L during 2014 and 40 to 2120 mg/L during 2018. According to WHO, the allowable limit of TH for drinking is 600 mg/L and the desirable limit is 300 mg/L. The Spatial Distribution of TH is as shown in *Figure 7*. The Total Hardness of the groundwater sample in the study area fell in the hard and very hard water category. Total Hardness means both temporary and permanent hardness. Hardness is a significant parameter in determining the need for industries and domestic purposes. Hard water does not produce much bad effect but it requires more detergent for cleaning and in some cases very hard water might be the reason for heart disease (Schoeller, 1965). The TH in mg/L is determined by *Equation 5* (Todd, 1959):

$$TH(mg / L) = 2 : 497Ca^{2+} + 4 : 115Mg^{2+} \quad (Eq.5)$$

Based on hardness groundwater is classified (Sawyer and McCarthy, 1967) and is presented in *Table 13*. In the study area, 22 samples were found in very hard class in 2014, whereas in 2018, 19 samples were found in very hard class. This reveals that Tuticorin experiences very hard water during both the years. High levels of hardness may affect water supply system, excessive detergent consumption and also health problem (Bhawan and Nagar, 2008).

Table 13. Classification based on hardness (Sawyer and McCarthy, 1967)

Total hardness as CaCO ₃ (mg/L)	Classification	2014		2018	
		Number of samples	Percentage of samples	Number of samples	Percentage of samples
<75	Soft	0	0	1	3
75–150	Moderately high	3	8	8	21
150–300	Hard	12	32	9	24
>300	Very Hard	22	58	19	50
Total		38	100	38	100

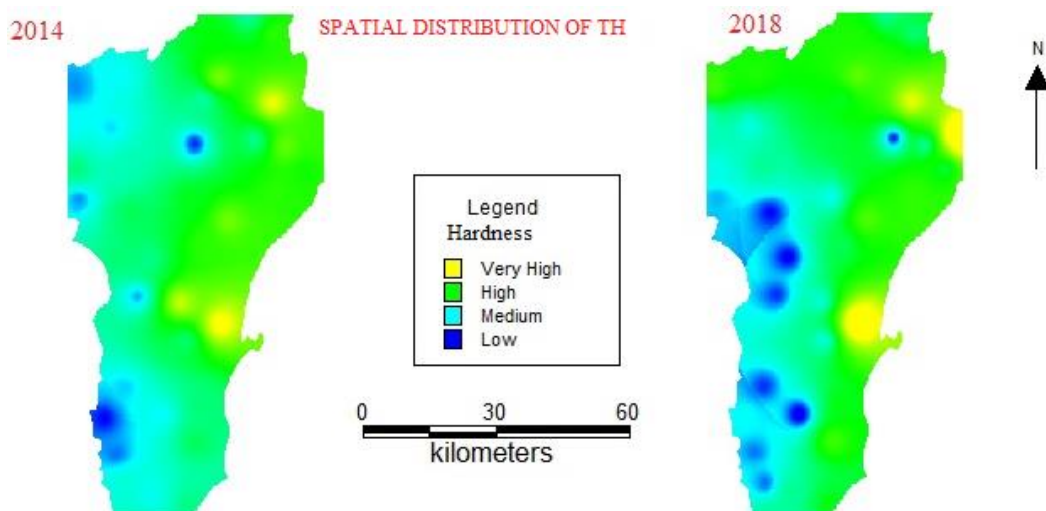


Figure 7. Spatial distribution of TH

Calcium

Calcium concentration is found to vary between 8-360 mg/L with a mean value of 74.53 mg/L for 2014 water samples and 8-272 mg/L with a mean value of 64.79 mg/L for 2018 samples. The allowable limit of calcium in groundwater is 200 mg/L as per WHO (2017). The Spatial Distribution of Calcium is shown in *Figure 8*. In 2014, 92% and in 2018, 97% of samples are up to the standard and only 8% samples exceed the permissible limit in 2014 and 3% samples exceed the permissible limit.

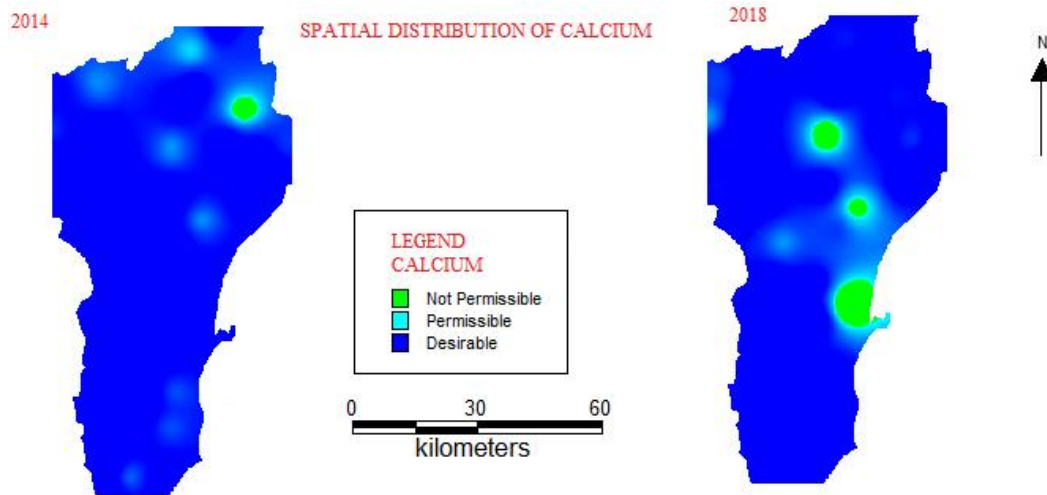


Figure 8. Spatial distribution of calcium

Magnesium

Magnesium vary from 10 to 175 mg/L with a mean value of 52.34 mg/L during the year 2014 and 5 to 493 mg/L with a mean value of 62.32 mg/L during the year 2018. The maximum allowable limit of magnesium in groundwater is 150 mg/L as per WHO (2017). The Spatial Distribution of Magnesium is shown in *Figure 9*. In 2014, only 3% of sample exceeds the permissible limit while in 2018 the 3% increased to 8% which revealed changes in water quality.

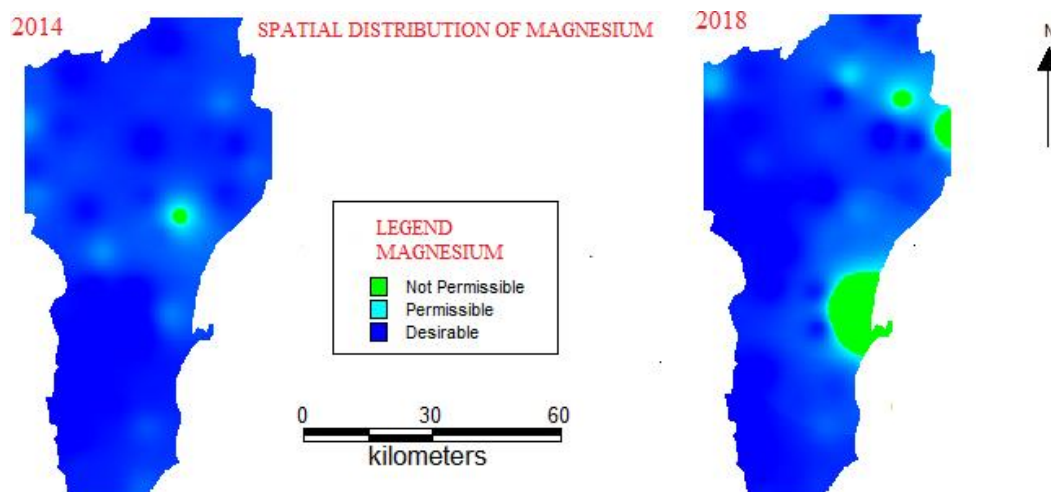


Figure 9. Spatial distribution of magnesium

Sodium

Sodium is found to vary from 10 to 552 mg/L with a mean value of 196.18 mg/L during the year 2014 and 7 to 1610 mg/L with a mean value of 265.55 mg/L during the year 2018. Sodium causes an increase in the hardness of soil as well as decrease its permeability (Tijani, 1994). The spatial distribution of sodium is shown in *Figure 10*. In 2014 and 2018 the high concentration of sodium is observed which may be due to saltwater intrusion.

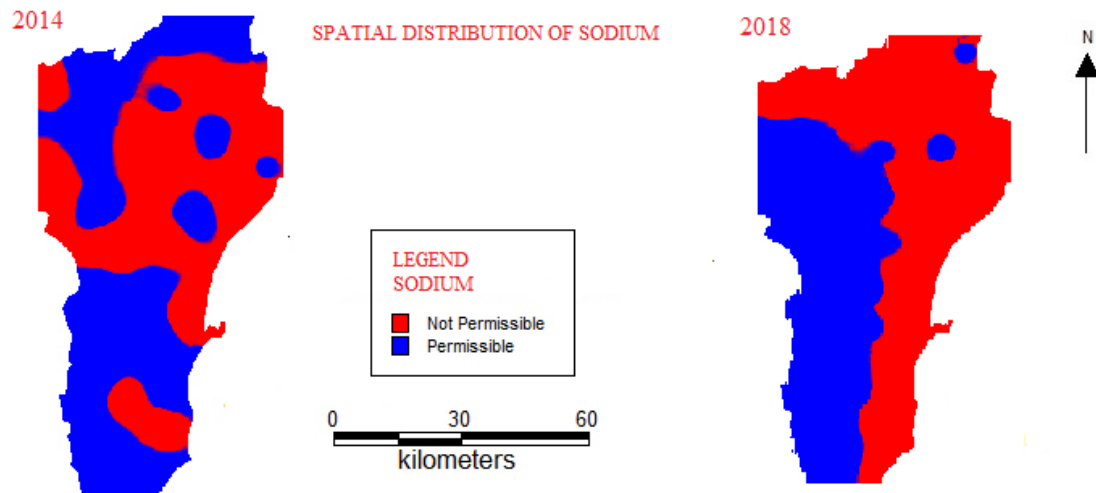


Figure 10. Spatial distribution of sodium

Potassium

Potassium ranges vary from 5 to 121 mg/L with a mean value of 24.84 mg/L during the year 2014 and 1 to 63 mg/L with a mean value of 14.71 mg/L during the year 2018. As per WHO (2017) standards, the allowable limit for potassium is 10 mg/L. The Spatial Distribution of Potassium is shown in *Figure 11*. Due to Salt pans, chemical fertilizer industries potassium concentration may be increased in the groundwater.

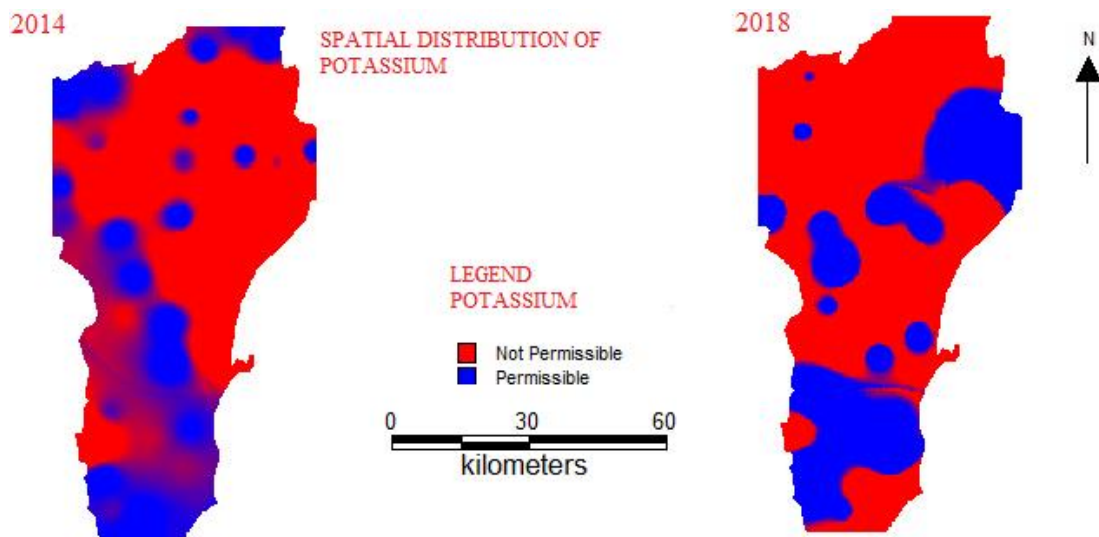


Figure 11. Spatial distribution of potassium

Bicarbonate

Bicarbonate ranges from 54 to 702 mg/l with a mean value of 311.63 mg/L during the year 2014 and 35 to 732 mg/L with a mean value of 378.93 mg/L during the year 2018. Bicarbonate concentrations are somewhat higher in the year 2018 compared to the year 2014 indicating the influence of carbonate due to weathering processes. There is a major variation observed in the spatial distribution of bicarbonate as shown in *Figure 12* which may be due to saltwater intrusion (Selvam et al., 2013; Srinivasamoorthy et al., 2011).

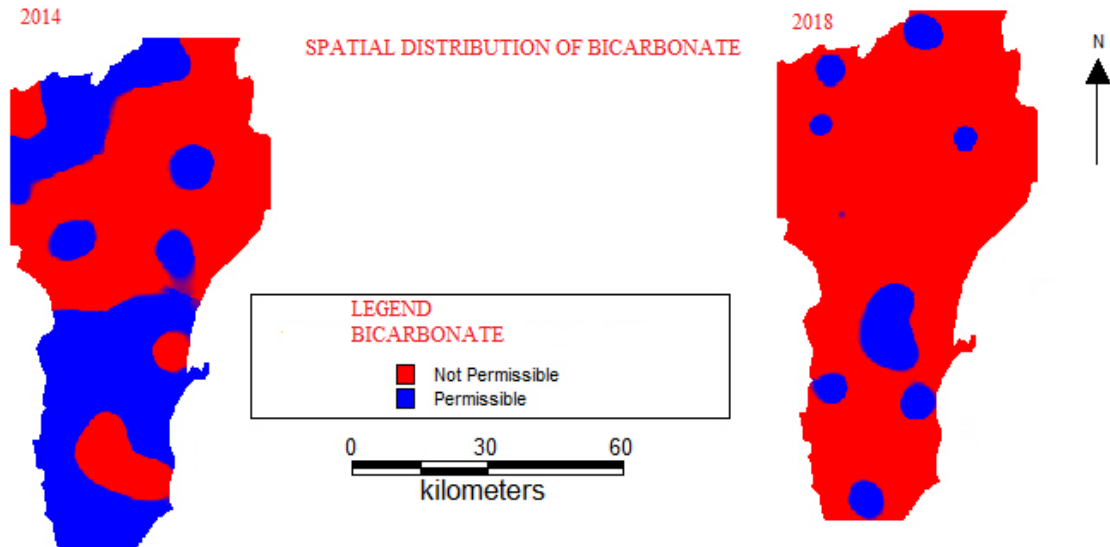


Figure 12. Spatial distribution of bicarbonate

Chloride

Chloride ranges from 7 to 865 mg/L with a mean value of 253.03 mg/L during the year 2014 and 7 to 1914 mg/L with a mean value of 328.34 mg/L during the year 2018. The allowable limit of Chloride is 600 mg/L. In Tuticorin 11% of sample exceed the permissible limit of chloride concentration in 2014. But in 2018 the percentage increases to 13%. Thus, high concentration of sodium and Chloride ions in groundwater may show a substantial effect of saltwater intrusion (Mondal et al., 2010). The Spatial Distribution of Chloride is shown in *Figure 13*. Higher concentration is noted during 2018 when compared with 2014 indicating domination of industrial activity and saltwater intrusion to the groundwater. High concentration of Chloride may be harmful to persons suffering from sicknesses of the heart and kidneys (Bhawan and Nagar, 2008).

Sulphate

Sulphate concentration vary from 10 to 624 mg/L with a mean value of 145.63 mg/L during the year 2014 and 6 to 1440 mg/L with a mean value of 194.08 mg/L during the year 2018. If the sulphate concentration exceeds allowable limit of 400 mg/L it will affect human organs. The sorting of groundwater based on sulphate is specified in *Table 2* and it is found that 5% of samples exceeded permissible limits during the year

2014 and 13% of samples are found to be exceeded the limits during the year 2018. Sulphate concentration in groundwater increases due to dissolution minerals and anthropogenic sources. The Spatial Distribution of Sulphate is shown in *Figure 14*.

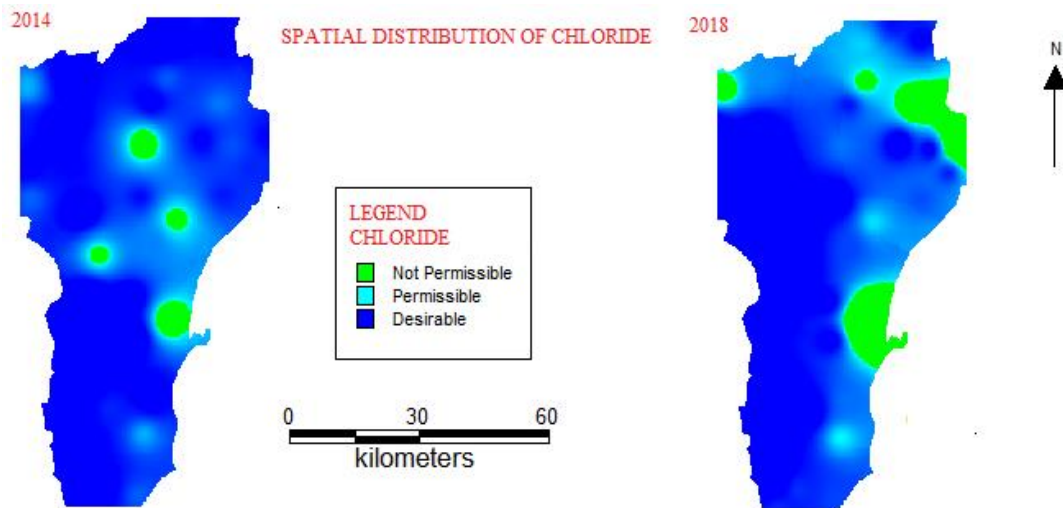


Figure 13. Spatial distribution of chloride

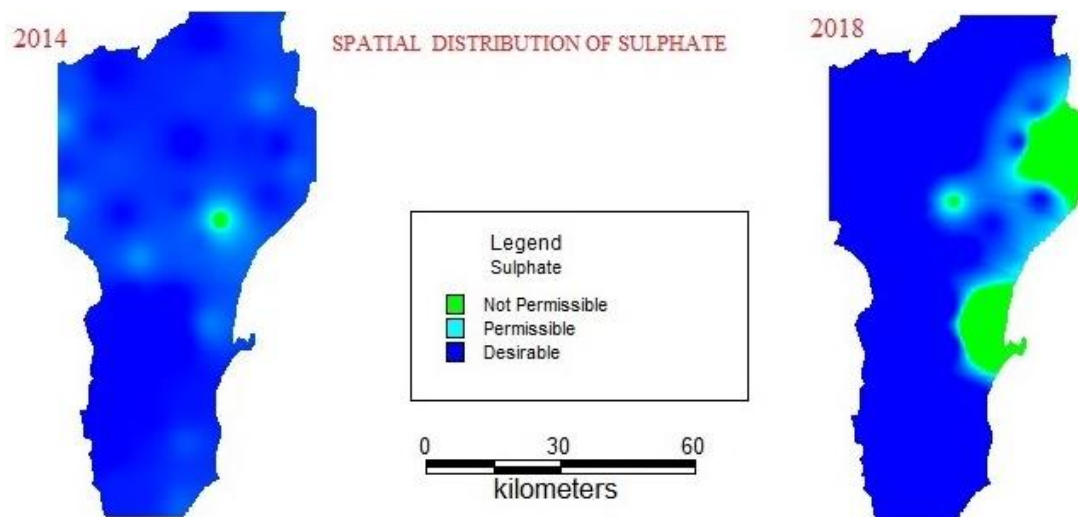


Figure 14. Spatial distribution of sulphate

Nitrate

Nitrate concentration vary from 1 to 73 mg/L with a mean value of 45.55 mg/L during the year 2014 and 1 to 55 mg/L with a mean value of 43.55 mg/L during the year 2018 allowable nitrate in drinking water as per WHO standards are 45 mg/L. The spatial distribution of nitrate is shown in *Figure 15*.

Fluoride

Fluoride concentration varies from 0 to 2 mg/L with a mean value of 0.64 mg/L during the year 2014 and 0 to 1 mg/L with a mean value of 0.46 mg/L during the year

2018. Allowable fluorides in drinking water as per WHO standards are 1.5 mg/L. Concentrations higher than allowable limit create many health problems (WHO, 2017). The spatial distribution of fluoride is shown in *Figure 16*.

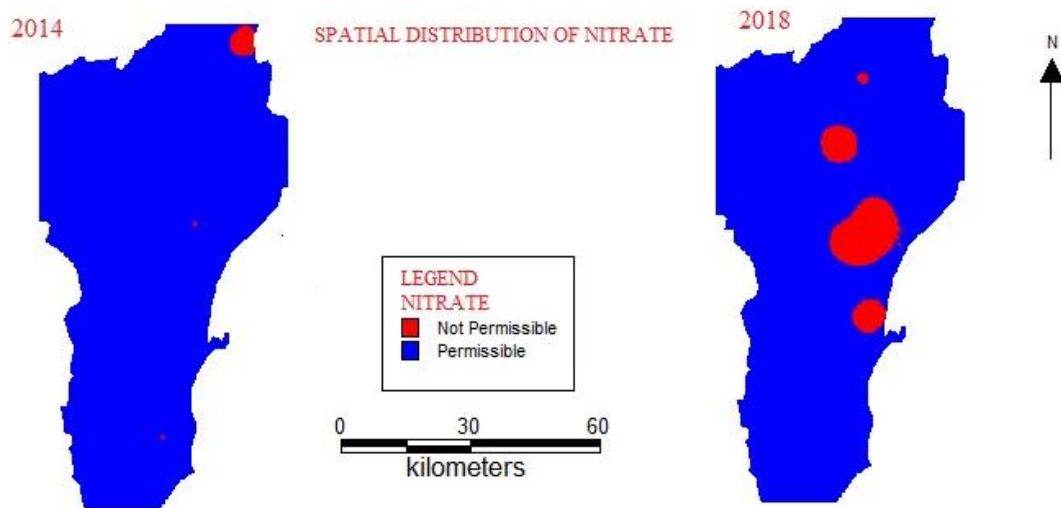


Figure 15. Spatial distribution of nitrate

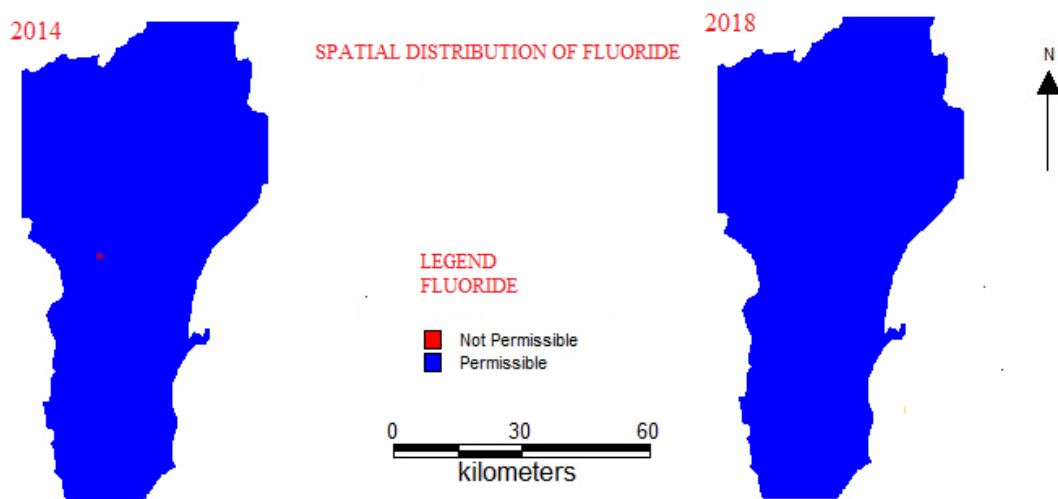


Figure 16. Spatial distribution of fluoride

According to salt concentration cations are characterized in ascending order as follows $\text{Na}^+ > \text{K}^+ > \text{Mg}^{2+} > \text{Ca}^{2+}$. From the above sorting it is clearly understood that Sodium and potassium concentration is prominent than the magnesium and calcium.

According to salt concentration anion are characterized in ascending order as follows $\text{HCO}_3^- > \text{Cl}^- > \text{SO}_4^{2-} > \text{F}^-$. From the above sorting, Cl and HCO_3^- showed a prominent role in Tuticorin than the concentrations of NO_3^- and F.

Piper plot

Statistical diagram such as Piper plot is used to understand about hydro chemical processes functioning in the groundwater. The Piper diagram is used to recognize

problems concerning the hydrogeochemical development of groundwater. The piper plot has three portions like two triangular portion and a diamond-shaped portion (Piper, 1944). The overall water quality is represented in the diamond-shaped field by extending the position of the plots in the triangular portion. Groundwater can be notable by their location, occupying certain spaces of the diamond-shaped portion. The experimental data obtained from the groundwater samples are plotted on a Piper trilinear diagram to understand the hydrogeochemical pattern in Tuticorin during the years 2014 and 2018.

The geochemical characteristics can be studied using Piper plot, which is separated into six sub groups (1) (Ca-HCO₃ type); (2) (Na-Cl type); (3) (mixed Ca-Na-HCO₃ type); (4) (mixed Ca-Mg-Cl type); (5) (Ca-Cl type) and (6) (Na-HCO₃ type). The diagram *Figure 17* exposed that the samples during 2014 found in the group of Na-Cl and mixed Ca-Mg-Cl type. But during 2018, Ca-HCO₃ type of water prevails in Tuticorin. Ca-Mg-Cl type of water falls under both years. It is detected that the alkalis (Na⁺ and K⁺) exceed the alkaline (Ca²⁺ and Mg²⁺) and strong acids exceed weak acids. During 2014 and 2018, strong acid dominant over weak acid and HCO₃³⁻ and Cl⁻ have influence equal to Na⁺, which indicates the severe saltwater intrusion occurred in Tuticorin.

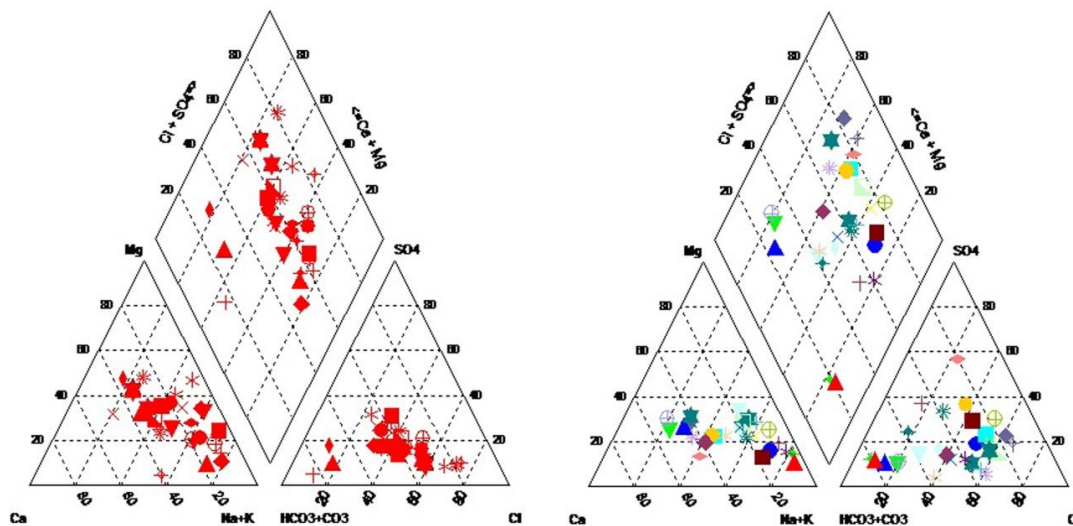


Figure 17. Piper plot during the years 2014 and 2018

Water quality index

The WQI for groundwater samples is exposed in *Tables 6* and *7*. Water collected from 38 observation wells are analysed for WQI. From the WQI value, it is found that villages like Keelairai, Kulathurterkku, Ottapidaram, Padanthapuli, Puthiyamputhur, Vilathikulam, Singathakuruchi, Vedanatham, Kachanavilai, Palangulam, Ariyanayagipuram, Srivaikundam, Thirukalur have showed improved water quality in 2018 compared with 2014. Water quality improvement may be due to the less withdrawal fresh groundwater and the rehabilitation of tanks. These villages located in the Taluk of Vilathikulam, Kovilpatti, Satankulam, Ettayapuram, Ottapidaram and Srivaikundam. The sample collected in villages present in Tuticorin Taluk like Melathattaparai, Marthadampatti have showed severe water quality deterioration

occurred from 2014 to 2018. Since the fresh groundwater extraction is more in Tuticorin due to industries saltwater intrusion occurs in the coastal aquifer. It is clearly portrayed from WQI method that the saltwater intrusion mainly in the coastal belt of Tuticorin and moves inward.

The spatial and attribute data are integrated for the creation of the spatial WQI map. The WQI Maps for the year 2014 and 2018 are depicted in *Figure 18*.

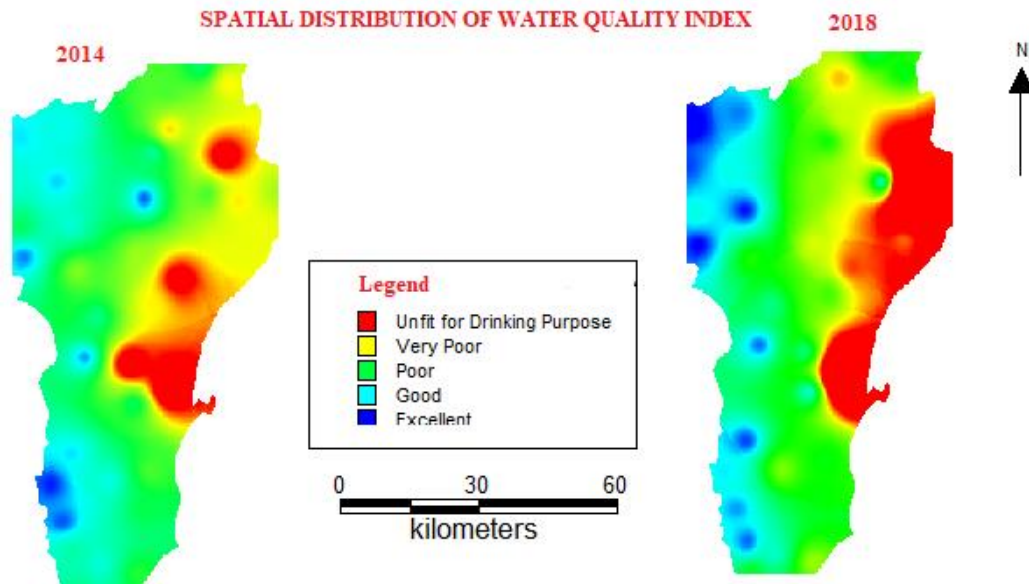


Figure 18. Water quality index map for the year 2014 and 2018

Comparison of WQI with the distance from sea

The computed WQI with respect to the distance of observation well from the sea is shown in *Figure 19*. From the figure it can be seen that water quality is poor in the observation wells found within 15 km from sea shore during the year 2018 whereas in 2014, observation wells found within 9 km are only affected. Similarly, in 2018 observation wells found within 7 km are unfit for drinking. Hence the saltwater intrusion has moved inward from the seashore to the distance of 15 km during 2018.

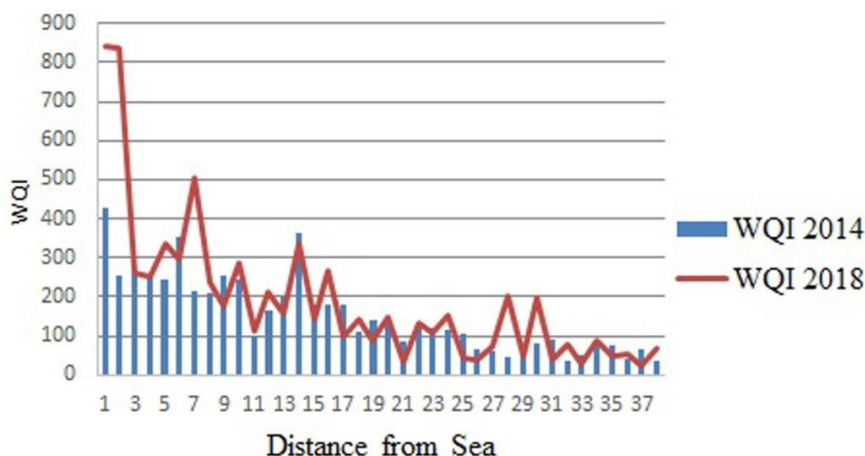


Figure 19. WQI with respect to the distance from sea

Model calibration

The model is calibrated for steady state and then for transient state. In a steady state calibration hydraulic conductivity and the recharge concentration are adjusted until hydraulic head measured using piezometer in 15 observation wells in April 2018 become close to the computed hydraulic heads. The calibrated results are depicted in *Figure 20*. Good match is found between observed and computed hydraulic head. For transient state calibration longitudinal and transverse dispersivity are changed to match observed salt concentration with computed salt concentration. Final calibrated value of longitude dispersivity is 30 m and transverse dispersivity is 4 m.

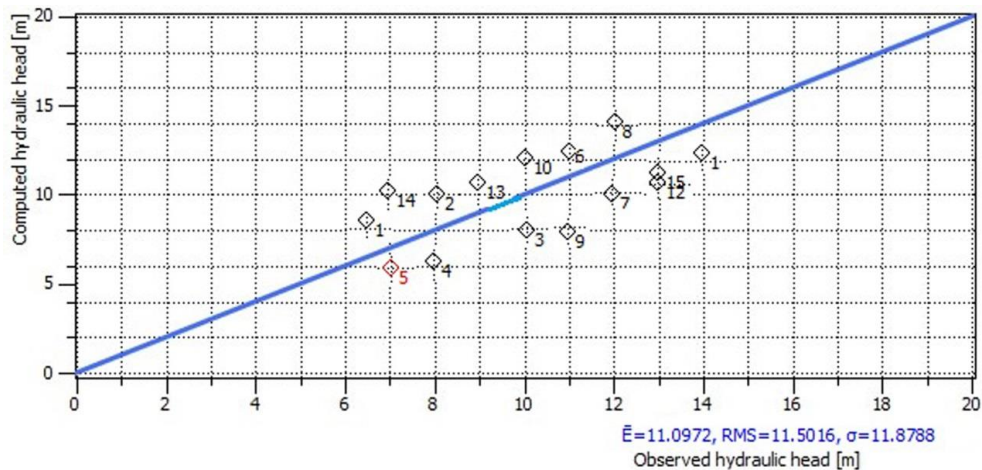


Figure 20. Comparison of measured and computed hydraulic head

Model verification

The Model developed is validated during the years 2000 to 2018 for the well located in Tuticorin by using data of salt concentration obtained from State Ground and Surface Water Resources Data Centre, Tamilnadu, India. A good match is found between the observed and simulated salt concentration in Tuticorin as shown in *Figure 21*.

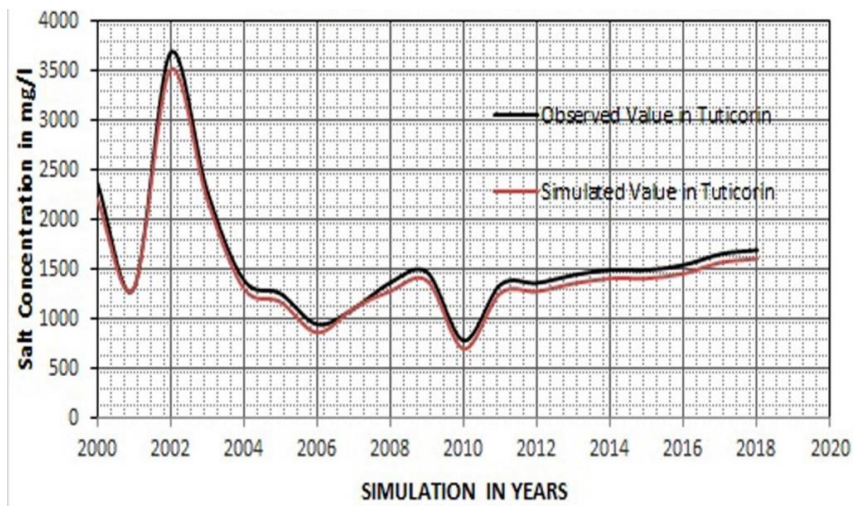


Figure 21. Model verification for the well in Tuticorin

Model simulation

The effect of Scenario A (Abstraction) Abstraction of saline groundwater using 15 pumping wells at a withdrawal rate of 1000 m³/day per well at a short distance of 1500 m from the shoreline is showed a significant change in salt concentration in Tuticorin as shown in *Figure 22*.

The effect of Scenario A (Abstraction) Abstraction of saline groundwater using 15 pumping wells at a withdrawal rate of 1000 m³/day per well at a short distance of 1500 m from the shoreline is showed a significant change in salt concentration in Tuticorin as shown in *Figure 22*. Simulated results of Scenario A (Abstraction) in the well in Tuticorin showed a decrease in groundwater salt concentration from 1600 mg/L in the year 2019 to 900 mg/L in the year 2030.

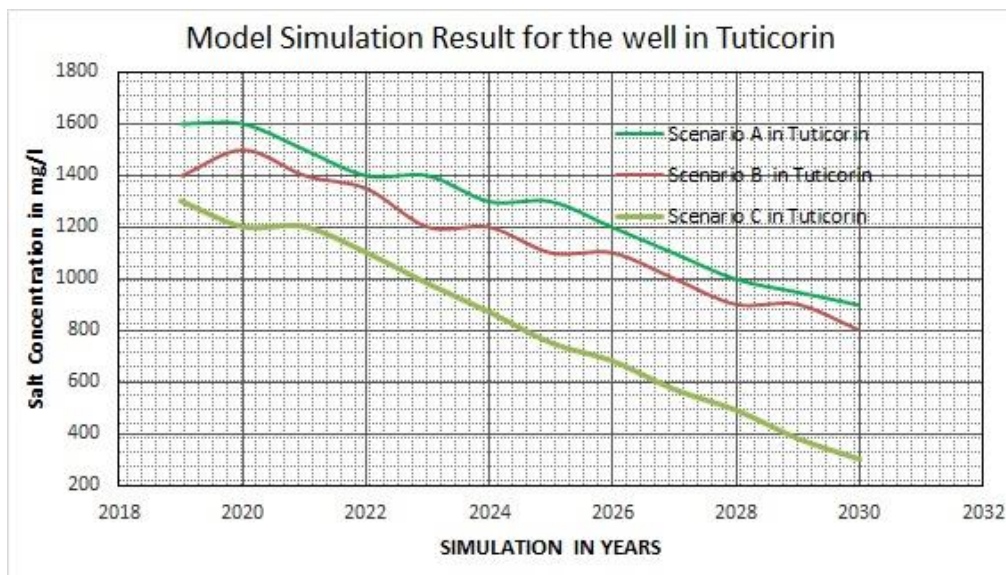


Figure 22. Simulation result for the well in Tuticorin

The Scenario B is the recharge of aquifer with treated saline water at the rate of 500 m³/day, showed to have significant impact than the pumping Scenario A as depicted in *Figure 22*. Simulated results of Scenario B (Recharge) in the well in Tuticorin exhibited a decrease in groundwater salt concentration from 1400 mg/L in the year 2019 to 800 mg/L in the year 2030.

But in Scenario C abstracting saline groundwater 1000 m³/day and recharge treated water at the rate of 500 m³/day showed good control over the salt water intrusion in Tuticorin as revealed in *Figure 22*. Simulated results of Scenario C (ADR) in the well in Tuticorin exposed a steady decline in groundwater salt concentration from 1300 mg/L in the year 2019 to 300 mg/l in the year 2030.

From the simulation result it is understood that ADR method is good to control water quality in the well from saltwater intrusion.

Discussion

From the Spatial analysis of water quality parameters, WQI method, Piper plot diagram, it is understood that the severe saltwater intrusion is occurred in Tuticorin. The

current pumping rate would further decline the water quality and can lead to the destruction of groundwater resources.

An attempt is made in the study to determine the distance of seawater intrusion based on WQI. The analysis results give better knowledge of zone of dispersion. Water Quality became very poor in the observation wells found within 15 km from sea shore in 2018. Hence the saltwater intrusion has moved inward from the seashore to a distance of 15 km. Pumping saline water from the zone of dispersion can reduce saltwater intrusion.

Several studies like Selvam et al. (2013) analysed the water quality parameter but the control measures not provided. In this research groundwater model is developed and three scenarios were applied to find the best method to minimise the seawater intrusion. The simulation results showed that ADR method is good to control from saltwater intrusion.

From the study, it is clearly depicted 15 pumping wells at a withdrawal rate of 1000 m³/day per well at a short distance of 1500 m from the shoreline and Recharge treated water at the rate of 500 m³/day required for the reduction, or displacement of the saline water towards the coast to eventually maintain or push the dispersion zone towards the coast is very important.

Conclusions

The effect of saltwater intrusion in coastal aquifer necessitates systematic investigation, especially when the extraction of groundwater in the coastal aquifer increases. The spatial analysis of groundwater using GIS, Water Quality Indices method, Piper plot diagram shows that the coastal aquifer is severely affected by saltwater intrusion. Potential intrusion of saltwater is studied with respect to distance of observation wells from seashore. In 2018 water quality in the observation wells located within 15 km from the Seashore is very much affected. Three different simulation scenarios namely Abstraction, Recharge and a combination of system were applied to the observation well located in Tuticorin to reduce the seawater intrusion. FEFLOW model was used to evaluate these methods adopted to reduce seawater intrusion. The simulation results of FEFLOW show that the method ADR performs better than using abstraction or recharge wells. Integrating field study with developed model to determine the site selection of recharge well is a possibility for future work.

REFERENCES

- [1] Azeez, P. A., Nadarajan, N. R., Mittal, D. D. (2000): The impact of a monsoonal wetland on groundwater chemistry. – *Pollution Research* 19(2): 249-255.
- [2] Barlow, P. M., Reichard, E. G. (2010): Saltwater intrusion in coastal regions of North America. – *Hydrogeology Journal* 18(1): 247-260.
- [3] Davis, S. N., Dewiest, R. J. M. (1966): *Hydrogeology*. Vol. 463. – Wiley, New York.
- [4] El Mokhtar, M., Chibout, M., El Mansouri, B., Chao, J., Kili, M., El Kanti, S. M. (2018): Modelling of the Groundwater flow and Saltwater Intrusion in the Coastal Aquifer of Fum Al Wad, Province of Laayouan, Morocco. – *International Journal of Geo Sciences* 9: 71-92.
- [5] Freeze, R. A., Cherry, J. A. (1979): *Groundwater*. – Prentice Hall, Englewood Cliffs.
- [6] Gebrehiwot, A. B., Tadesse, N., Jigar, E. (2011): Application of water quality index to assess suitability of groundwater quality for drinking purposes in Hantebet watershed,

- Tigray, Northern Ethiopia. – *ISABB Journal of Food and Agricultural Sciences* 1(1): 22-30.
- [7] Handa, B. K. (1969): Description and classification of media for hydro-geochemical investigations. – Symposium on Groundwater Studies in Arid and Semiarid Regions, Roorkee.
- [8] Hussain, M. S., Javadi, A. A., Ahangar-Asr, A., Farmani, R. (2015): A surrogate model for simulation - optimization of a aquifer systems subjected to seawater intrusion. – *Journal of Hydrology* 523: 542-554.
- [9] Idowu, T. E., Ezekiel, N. M., Korowe, M. (2016): Seawater intrusion vulnerability assesment of a coastal aquifer: north coast of Mombasa, Kenya as a case study. – *International Journal of Engineering Research and Application* 6(8): 37-45.
- [10] Jebastina, N., Arulraj, G. P. (2017): GIS based assessment of groundwater quality in Coimbatore District, India. – *Journal of Environmental and Analytical Toxicology* 7(3): 1-9.
- [11] Jebastina, N., Prince Arulraj, G. (2016): Contamination analysis of groundwater in Coimbatore District, India: a statistical approach. – *Environmental Earth Sciences* 75: 1447.
- [12] Kalpana, G. R., Nagarajappa, D. P., Sundar, K. S., Suresh, B. (2014): Determination of groundwater quality index in Vidyanagar, Davanagere City, Karnataka State, India. – *International Journal of Engineering and Innovative Technology (IJEIT)* 3(12): 90-99.
- [13] Mondal, N. C., Singh, V. P., Singh, V. S., Saxena, V. K. (2010): Determining the interaction between groundwater and saline water through groundwater major ions chemistry. – *Journal of Hydrology* 388(1-2): 100-111.
- [14] Piper, A. M. (1944): A graphic procedure in the geochemical interpretation of water-analyses. – *EOS, Transactions American Geophysical Union* 25(6): 914-928.
- [15] Ramesh, S., Sukumaran, N., Murugesan, A. G., Rajan, M. P. (2010): An innovative approach of drinking water quality index—A case study from Southern Tamil Nadu, India. – *Ecological Indicators* 10(4): 857-868.
- [16] Rao, S. V. N., Sreenivasulu, V., Bhallamudi, S. M., Thandaveswara, B. S., Sudheer, K. P. (2004): Planning groundwater development in coastal aquifers. – *Hydrological Sciences Journal* 49(1): 155-170.
- [17] Sawyer, C., McCarthy, P. (1967): *Chemistry for Sanitary Engineering*. – McGraw-Hill, New York.
- [18] Schoeller, H. (1965): *Qualitative Evaluation of Groundwater Resources. Methods and Techniques of Groundwater Investigations and Development*. – UNESCO 5483, Paris.
- [19] Selvam, S., Manimaran, G., Sivasubramanian, P. (2013): Hydrochemical characteristics and GIS-based assessment of groundwater quality in the coastal aquifers of Tuticorin corporation, Tamilnadu, India. – *Applied Water Science* 3(1): 145-159.
- [20] Sener, E., Sener, S., Davraz, A. (2009): Assessment of aquifer vulnerability based on GIS and DRASTIC methods: a case study of the Senirkent-Uluborlu Basin (Isparta, Turkey). – *Hydrogeology Journal* 17(8): 2023.
- [21] Serrekawo, N., Karuppanan, S. (2018): Groundwater quality assessment using water quality index in Modjo River Basin, Central Ethiopia. – *Journal of African Earth Sciences* 147: 300-311.
- [22] Sherif, M., Kacimov, A. (2008): Pumping of brackish and saline water in coastal aquifers: an effective tool for alleviation of seawater intrusion. – *Proceeding of 20th SWIM, Naples, Florida, USA*.
- [23] Sherif, M. M., Hamza, K. I. (2001): Mitigation of seawater intrusion by pumping brackish water. – *Transport in Porous Media* 43(1): 29-44.
- [24] Song, T., Kim, K. (2009): Development of a water quality loading index based on water quality modeling. – *Journal of Environmental Management* 90(3): 1534-1543.

- [25] Srinivas, Y., Oliver, D. H., Raj, A. S., Chandrasekar, N. (2013): Evaluation of groundwater quality in and around Nagercoil town, Tamilnadu, India: an integrated geochemical and GIS approach. – *Applied Water Science* 3(3): 631-651.
- [26] Srinivasamoorthy, K., Nanthakumar, C., Vasanthavigar, M., Vijayaraghavan, K., Rajivgandhi, R., Chidambaram, S., Anandhan, P., Manivannan, R., Vasudevan, S. (2011): Groundwater quality assessment from a hard rock terrain, Salem district of Tamilnadu, India. – *Arabian Journal of Geosciences* 4(1-2): 91-102.
- [27] Stigter, T. Y., Ribeiro, L., Dill, A. C. (2006): Application of a groundwater quality index as an assessment and communication tool in agro-environmental policies—Two Portuguese case studies. – *Journal of Hydrology* 327(3-4): 578-591.
- [28] Tavassoli, S., Mohammadi, F. (2017): Groundwater quality assessment based on WQI and its vulnerability to saltwater intrusion in a coastal city, Iran. – *Journal of Geo Science and Environment Protection* 5: 88-98.
- [29] Thomas, A., Eldho, T. I., Rastogi, A. K. (2016): Simulation of seawater intrusion in coastal confined aquifer using a point collocation method based mesh free model. – *Journal of Water Resource and Protection* 8: 534-549.
- [30] Tijani, M. N. (1994): Hydrogeochemical assessment of groundwater in Moro area, Kwara State, Nigeria. – *Environmental Geology* 24(3): 194-202.
- [31] Todd, D. K. (1959): *Groundwater Hydrology*. – John Wiley and Sons, New York.
- [32] Todd, D. K. (1974): *Salt-Water Intrusion and Its Control*. – *Journal-American Water Works Association* 66(3): 180-187.
- [33] Todd, D. K. (1980): *Groundwater Hydrology*. Second Edition. – John Wiley and Sons, New York.
- [34] World Health Organization (2017): *Guidelines for Drinking-Water Quality: First Addendum to the Fourth Edition*. – WHO, Geneva.